

Bi-modal microstructure in a powder metallurgical ferritic steel

LIU Feng, LIU Yong, WU Hong, FANG Jing-hua, ZHAO Da-peng, ZHANG Liu-jie, LIU Dong-hua

State Key Laboratory of Powder Metallurgy, Central South University, Changsha 410083, China

Received 7 January 2011; accepted 26 May 2011

Abstract: Ferritic steel with a nominal composition of Fe–14Cr–3W–0.42Ti–0.32Y was prepared by mixing gas-atomized prealloyed powder and mechanically alloyed powder. The microstructure is much different from other ferritic steels with the same composition and prepared via only mechanically alloyed powder. A bi-modal structure, which consists of pure ferritic grains and martensitic grains, was obtained after hot forging and air cooling. A phase transformation of $\alpha_{\text{bcc}} \rightarrow \gamma_{\text{fcc}} \rightarrow \alpha'_{\text{bcc}}$ was also discovered in microstructural observation. The bi-modal microstructure shows a good combination of high strength and high ductility.

Key words: ferritic steel; powder metallurgy; phase transformation; bi-modal microstructure; mechanical property

1 Introduction

The ferritic steels are considered potential candidates for elevated temperature applications in fusion reactors [1–3] and fission reactors, because of their high thermal conductivity, low thermal expansion coefficient, and low void swelling. Recently, a 14CrYWT ferritic stainless steel has been extensively studied, due to its high creep strength, irradiation resistance and high temperature stability [4–6].

The alloy was commonly prepared by using mechanically alloyed powder. Firstly, Fe–Cr–W pre-alloyed powder was prepared by gas atomization, and then the powder was mechanically alloyed with Y_2O_3 powder. Finally, the powder was sealed, vacuumed and hot extruded or hot isothermal pressed. The microstructure is uniform ferritic phase, with Y–Ti–O nanoclusters at very fine scale [7]. Mechanical alloying alone is not a good method for large-scaled production, and this might be the main obstacle for the engineering application of this steel.

The authors thus tried to modify the manufacturing process, by mixing Fe–Cr–W pre-alloyed powder with mechanically alloyed Fe–Cr–W–Ti–Y–O powder. In doing so, an unexpected microstructure and phase transformation were produced. This work thus aims at studying the microstructural evolution in this specially

prepared material, and their mechanical properties as well.

2 Experimental

The nominal composition (mass fraction) of the alloy used in the experiment was: Cr 14%, W 3%, Ti 0.42%, Y 0.32%, and residual Fe. The actually measured mass fractions of C and O in the bulk form were 0.036% and 0.063%, respectively. The argon gas atomized Fe–14Cr–3W pre-alloyed powders were mechanically alloyed with 1.6% YH_2 and 2.1% TiH_2 powders in a high-energy planet type ball mill for 24 h. Mechanical alloying was conducted in a Pulverisette-5 planetary ball mill (ball to powder mass ratio 8:1, rotation speed 350 r/min and 0.5% alcohol as process control agent). And then the MAed powder was mixed with Fe–14Cr–3W pre-alloyed powders to get the aimed chemical composition, which was Fe–14Cr–3W–0.42Ti–0.32Y. The mixed powder was sealed in a steel can, vacuumed to 10^{-2} Pa and consolidated by hot forging at 1273 K. Samples with dimensions of 5 mm×5 mm×4 mm were cut from the as-forged steel, and heat treated in two different ways, which were marked as H1 and H2, respectively. H1 was to anneal the as-forged samples at 1073, 1273 and 1473 K for 1 h, and air cooling. H2 was to anneal the as-forged samples at 1073, 1273 and 1473 K for 1 h, and furnace cooling. Vickers

microhardness was measured by using MICROMET 5104 at a load of 100 mN. The phase constitutions of the samples were determined by using a Rigaku D/max 2550VB+ X-ray diffractometer (XRD), with a Cu K_{α} target, scanning at a voltage of 40 kV and a speed of 8 ($^{\circ}$)/min. The phase transformation in the heat treatment was studied by NETZSCH STA 449C differential scanning calorimeter (DSC). The as-forged samples were heated up with 10 K/s to 1473 K. A JEOL-2010 transmission electron microscope was used for more detailed study on the microstructures. Disk specimens were spark eroded from the bulk, polished with emery paper and then electro-polished by twin-jet with a solution containing 5% $HClO_4$ and 95% CH_3OH (volume fraction). The tensile specimen was of a small sheet-type with a gauge section of 8 mm \times 3 mm and 1 mm in thickness.

3 Results

3.1 Microstructures

Figure 1 shows the optical micrographs of the alloys after different heat treatments. Figures 1(a) and (b) show that recrystallization has occurred at 1073 K, and no new phase except the ferrite exists in the alloy. Figures 1(c) and (d) show that two kinds of grains with different morphologies formed in the sample. One kind of grains is very clean inside without precipitates, while the other has a rough morphology with lath-like phases inside. Moreover, the rough grains are rather smaller compared with the clean grain in size, which is about 20 μm . The microhardness of the rough grains was measured as HV687, while that of the clean grain was just HV203. After furnace cooling, the microstructure becomes

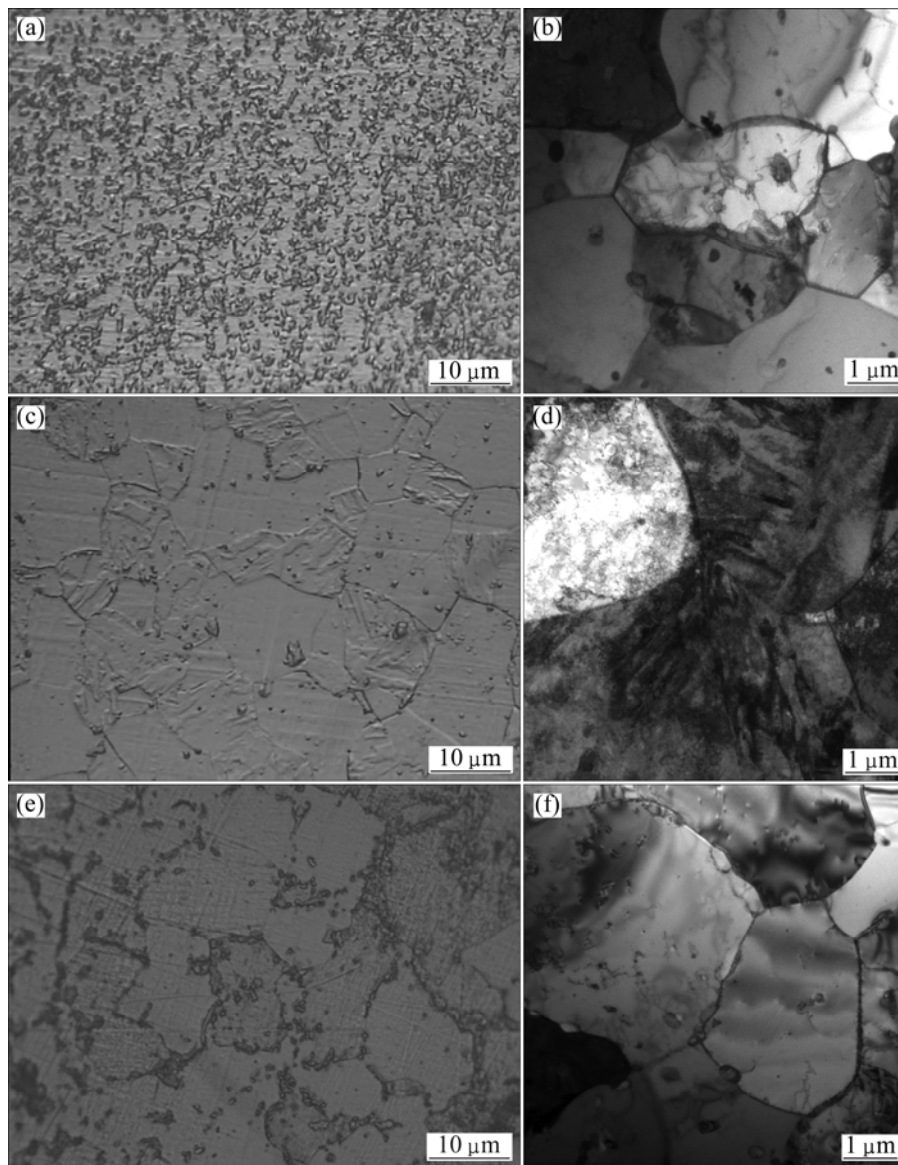


Fig. 1 Optical micrographs of alloys after different heat treatments: (a), (b) At 1073 K for 1 h and air cooling; (c), (d) At 1273 K for 1 h and air cooling; (e), (f) At 1273 K for 1 h and furnace cooling

homogeneous, as shown in Figs. 1(e) and (f). The only difference in the whole heat treatment process between the samples in Figs. 1(a) and (e) is the cooling routine. The sample in Fig. 1(a) was air quenched to room temperature, while the sample in Fig. 1(e) was furnace cooled to room temperature. So, it is distinctly that the lath microstructure in the alloy must occur in the cooling procedure due to the different cooling rate, i.e., the cooling manner (furnace cooling or air cooling). As well as there was no phase transformation in the sample air cooled at 1073 K, it can be seen that the air cooled temperature is also an important factor in the phase transformation.

3.2 Phase analysis and martensitic characterization

XRD patterns in Figs. 2 (a) and (b) show that the elements Ti and Y have been dissolved in the matrix after mechanically alloying. And all samples have almost the same BCC structure. It is well known that the BCC structure in steels is either ferritic or martensitic phase. Since the nominal composition of the steel is in the range of ferritic region, the main phase in samples should be ferrite. The morphology in Fig. 1(b) is in consistence with martensitic phase. So, in Fig. 2(d) some martensitic peaks may exist. However, due to almost the same lattice parameters, there should have additional peaks to be the martensitic phase. Thus the air-cooled samples were with bimodal structure that is a mixture of ferritic and martensitic phases.

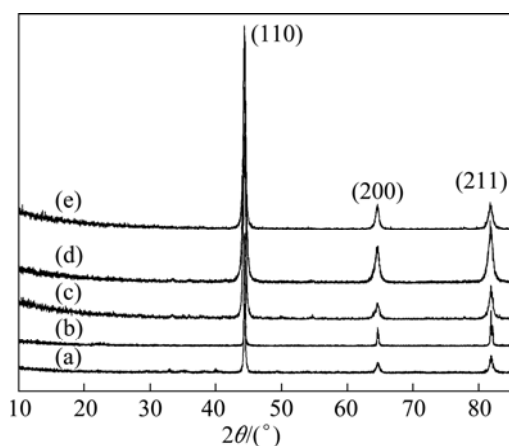


Fig. 2 XRD patterns of samples: (a) Fe–14Cr–3W prealloyed powder; (b) MAed powder; (c) After treatment at 1073 K for 1 h and air cooling; (d) After treatment at 1273 K for 1 h and air cooling; (e) After treatment at 1273 K for 1 h and furnace cooling

TEM observations were carried out in order to characterize the microstructures in details. In most cases, three kinds of phases were observed as shown in Fig. 3, i.e., ferrite (the white region), martensite (the lath-like grain) and retained austenite (between the lath

boundaries). And the martensite lath has a high density of dislocation. MCMAHON [8] reported that the typical microstructure in low carbon steel was lath martensite and retained austenite between lath boundaries. It was further observed that the growth of prior austenite at an early stage of the transformation always starts directly from a grain boundary of ferrite [9]. So, it is deduced that the phase transformation of ferrite to austenite occurred in the heating process and then austenite transformed to martensite in the quenching process. After air quenching, there also contained a small amount of retained austenite shown in Fig. 3. According to selective area electron diffraction pattern, the orientation relationship between retained austenite and BCC martensite is $(\bar{6}24)_\gamma // (011)_{\alpha'} \cdot [245]_\gamma // [011]_{\alpha'}$.

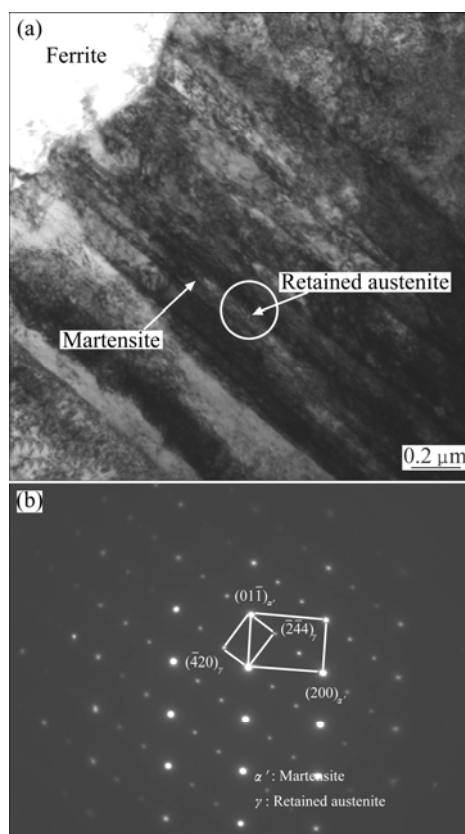


Fig. 3 TEM bright field image (a) and selective area electron diffraction pattern (b) of martensite lath after isothermal heat treatment at 1273 K for 1 h and subsequently air cooling

3.3 Phase transformation

In order to further examine the mechanism of martensitic transformation in the ferritic steel, a DSC (differential scanning calorimeter) measurement was carried out. In Fig. 4, there is an endothermic peak at 984.7 K, corresponding to the magnetic transition from a ferromagnetic state to a paramagnetic state. And the endothermic peak at 1198.4 K is considered the A_{c1} temperature, i.e., the temperature of the transformation from ferrite to austenite [10]. So, it can be confirmed that

there are some austenite phases formed in the heating process, then which were transformed to martensites in the air quenching process.

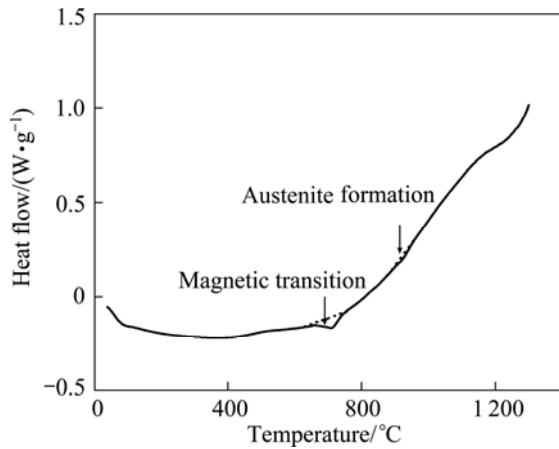


Fig. 4 DSC curves measured on as-forged specimen

3.4 Mechanical properties

Figure 5 shows the mechanical properties of samples with different cooling processes at the same heat treatment temperature. The ultimate tensile strength has raised up to over 50% from 592 MPa to 910 MPa, whereas, the plastic properties only decreased moderately. It is evident that the martensitic phase plays an important role in strengthening of the ferritic steel at ambient temperature.

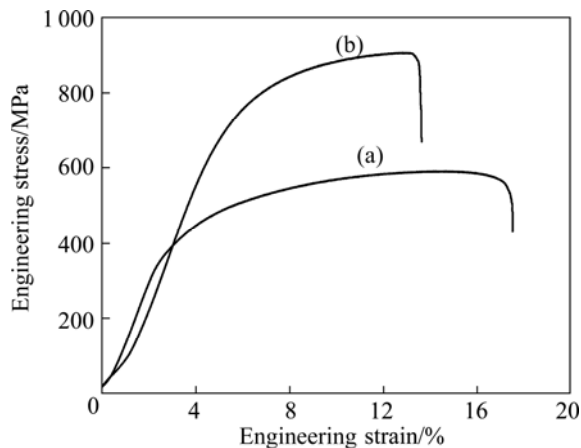


Fig. 5 Mechanical properties of samples at room temperature: (a) Sample treated at 1273 K for 1 h and furnace cooled; (b) Sample treated at 1273 K for 1 h and air cooled

4 Discussion

Since the nominal composition of the alloy lies in the ferrite phase region, it is hard to understand the occurrence of austenite and martensite. The main reason is attributed to the compositional deviation and inhomogeneity in the powder mixtures. As mentioned before, there was a 0.036% C (mass fraction)

contamination. According to Fe–C phase diagram and other studies [11–12], the small addition of C will induce martensite formation, which is always in a lath-like morphology. On the other hand, contamination of Fe during MA process may also occur, and results in the decrease of Cr in MAed powder, and deviation of the chemical composition to the γ -phase region. The actually measured mass fraction of Cr in the MAed powders is about 12.7%. Therefore, the ferrite grains in the microstructure come from the pre-alloyed Fe–Cr–W powder, while the martensitic grains come from the MAed powder. During high temperature consolidation and heat treatment, the chemical composition in local areas may further change due to diffusion and segregation.

The solid solubility of carbon in the α -ferrite is just 0.0218% at 1273 K, and the excess interstitial carbon atoms would diffuse along the grain boundaries during the heat treatment [13]. The diffusion process may result in the enrichment of carbon element in grain boundaries, and also induce the segregation of Cr, due to the fact that Cr atom has a strong affinity with carbon [14]. Thus, the regions nearby ferrite grains could have a composition with high C content and Cr content lower than 14%, and martensitic transformation occurs at a fast enough cooling rate, e.g., air cooling [15].

In summary, a bimodal microstructure, consisting of ferritic grains and martensitic grains, can be obtained by using mixtures of gas-atomized Fe–14Cr–3W powder and MAed Fe–14Cr–(Ti–Y–O) powder, followed by air cooling. The formation of martensitic structure is due to the chemical compositional inhomogeneity and deviation in local areas, during both MA process and subsequent heat treatment. The bi-modal microstructure shows a better combination of high strength and high ductility.

5 Conclusions

1) A bi-modal microstructure has been discovered, which is different from conventional ferrite structure. The phase transformation of $\alpha_{\text{bcc}} \rightarrow \gamma_{\text{fcc}} \rightarrow \alpha'_{\text{bcc}}$ has been proved.

2) It is shown that the room temperature mechanical property of the bi-modal microstructure is much better than homogeneous ferrite structure.

References

- [1] KLUEH R L, MAZIASZ P J, KIM I S, HEATHERLY L, HOELZER D T, HASHIMOTO N, KENIK E A, MIYAHARA K. Tensile and creep properties of an oxide dispersion-strengthened ferritic steel [J]. *J Nucl Mater*, 2002, 307–311(Part 1): 773–777.
- [2] LIU Yong, FANG Jing-hua, LIU Dong-hua, LU Zhi, LIU Feng, CHEN Shi-qi, LIU C T. Formation of oxides particles in ferritic steel by using gas-atomized powder [J]. *J Nucl Mater*, 2010, 396: 86–93.

- [3] MILLER M K, HOELZER D T, KENIK E A, RUSSELL K F. Stability of ferritic MA/ODS alloys at high temperatures [J]. *Intermetallics*, 2004, 13: 387–392.
- [4] LIU Dong-hua, LIU Yong, ZHAO Da-peng, LIU Zu-ming, HAN Yun-juan. Effect of addition manner of oxygen on mechanical properties of iron-based alloy 14YWT [J]. *The Chinese Journal of Nonferrous Metals*, 2010, 20(5): 846–851. (in Chinese)
- [5] ZHANG Ning-yi, LIU Yong, LIU Feng, LIU Zu-ming, FANG Jing-hua, LIU Dong-hua, WEN Yu-ren. Effects of annealing temperature on microhardness and microstructure of hot-extruded superalloy Fe13CrWTiY [J]. *Materials Science and Engineering of Powder Metallurgy*, 2008, 13: 245–248. (in Chinese)
- [6] SCHNEIBEL J H, LIU C T, MILLER M K, MILLS M J, SAROSI P, HEILMAIER M, STURM D. Ultrafine-grained nanocluster-strengthened alloys with unusually high creep strength [J]. *Scripta Mater*, 2009, 61(8): 793–796.
- [7] MILLER M K, RUSSELL K F, HOELZER D T. Characterization of precipitates in MA/ODS ferritic alloys [J]. *J Nucl Mater*, 2006, 351(1–3): 261–268.
- [8] MCMAHON G T. Development of economical tough ultrahigh-strength Fe–Cr–C steel [C]// Proc 3rd Int Conf on Strength of Metals and Alloys, 1973, 20–25: 180.
- [9] BELADI H, KELLY G L, SHOKOUHI A, HODGSON P D. The evolution of ultrafine ferrite formation through dynamic strain-induced transformation [J]. *Mater Sci Eng A*, 2004, 371 (1–2): 343–352.
- [10] TOKUNAGA T, HASEGAWA K, MASUYAMA F. Phase transformation behavior of Grade 91 ferritic steel [J]. *Mater Sci Eng A*, 2009, 510–511: 158–161.
- [11] OKAMOTO H. Phase diagrams of binary alloy [M]. University of Michigan: ASM International, 1993: 472–473.
- [12] RAO B V N, THOMAS G. Structure-property relations and the design of Fe–4Cr–C Base structural steels for high strength and toughness [J]. *Metall Trans A*, 1980, 11: 441–457.
- [13] XU Zu-yao, LI Xue-ming. Diffusion of carbon during the formation of low-carbon martensite [J]. *Acta Mater Sinica*, 1983, 19(2): 7–144. (in Chinese)
- [14] KIM J K, LEE B J, LEE B H, KIM Y H, KIM K Y. Intergranular segregation of Cr in Ti-stabilized low-Cr ferritic stainless steel [J]. *Scripta Mater*, 2009, 61(12): 1133–1136.
- [15] TSAI M C, CHIOU C S, DU J S, YANG J R. Phase transformation in AISI 410 stainless steel [J]. *Mater Sci Eng A*, 2002, 332: 1–10.

一种粉末冶金铁素体钢中的双组态结构

刘 锋, 刘 咏, 吴 宏, 方京华, 赵大鹏, 张刘杰, 刘东华

中南大学 粉末冶金国家重点实验室, 长沙 410083

摘 要: 采用混合预合金粉末和球磨粉末的方法, 制备一种具有双组态结构的铁素体合金钢, 其名义成分为 Fe–14Cr–3W–0.42Ti–0.32Y。其微观组织与成分相同但是采用全球磨粉末成形的铁素体钢有明显的区别。通过热锻、空冷之后, 该合金具有铁素体晶粒和马氏体晶粒混合构成的双组态结构。通过微观组织研究发现了在该合金中发生了局部的 $\alpha_{\text{bcc}} \rightarrow \gamma_{\text{fcc}} \rightarrow \alpha'_{\text{bcc}}$ 相变。同时, 这种双组态结构能够较好地均衡合金的强度和韧性。

关键词: 铁素体钢; 粉末冶金; 相变; 双组态结构; 力学性能

(Edited by YANG Hua)